



HAL
open science

High-precision $^{40}\text{Ar}/^{39}\text{Ar}$ dating of Australasian tektites associated with bifacial tools in the Bose Basin (Xiaomei and Fengshudao sites), South China and in Vietnam (Go Da and Roc Tung 1 sites)

Véronique Michel, Fred Jourdan, Marie-Hélène Moncel, Bernard Gratuze, Guanjun Shen, Wei Wang, Celia Mayers, Adam Frew, Dominique Cauche, Patricia Valensi, et al.

► To cite this version:

Véronique Michel, Fred Jourdan, Marie-Hélène Moncel, Bernard Gratuze, Guanjun Shen, et al.. High-precision $^{40}\text{Ar}/^{39}\text{Ar}$ dating of Australasian tektites associated with bifacial tools in the Bose Basin (Xiaomei and Fengshudao sites), South China and in Vietnam (Go Da and Roc Tung 1 sites). *Quaternary Science Reviews*, 2024, 346, pp.109065. 10.1016/j.quascirev.2024.109065 . hal-04792396

HAL Id: hal-04792396

<https://hal.science/hal-04792396v1>

Submitted on 20 Nov 2024

HAL is a multi-disciplinary open access archive for the deposit and dissemination of scientific research documents, whether they are published or not. The documents may come from teaching and research institutions in France or abroad, or from public or private research centers.

L'archive ouverte pluridisciplinaire **HAL**, est destinée au dépôt et à la diffusion de documents scientifiques de niveau recherche, publiés ou non, émanant des établissements d'enseignement et de recherche français ou étrangers, des laboratoires publics ou privés.

1 <https://doi.org/10.1016/j.quascirev.2024.109065>

2

3 **High-precision $^{40}\text{Ar}/^{39}\text{Ar}$ dating of Australasian tektites associated with**
4 **bifacial tools in the Bose Basin (Xiaomei and Fengshudao sites), South China**
5 **and in Vietnam (Go Da and Roc Tung 1 sites).**

6

7 Véronique Michel^{a,b,*}, Fred Jourdan^c, Marie-Hélène Moncel^d, Bernard Gratuze^e, Guanjun
8 Shen^f, Wei Wang^g, Celia Mayers^c, Adam Frew^c, Dominique Cauche^h, Patricia Valensi^d, Sylvain
9 Gallet^b, Anatoly P. Dereviankoⁱ, Alexander V. Kandybaⁱ, Sergey A. Gladyshevⁱ, Henry de
10 Lumley^h

11 ^a *Université Côte d'Azur, CNRS, CEPAM, Nice, France*

12

13 ^b *Université Côte d'Azur, CNRS, Observatoire de la Côte d'Azur, IRD, Géoazur, Valbonne,*
14 *France*

15

16 ^c *Western Australian Argon Isotope Facility, School of Earth and Planetary Sciences, John de*
17 *Laeter Centre, Space Science and Technology Centre, Curtin University, Perth, WA,*
18 *Australia.*

19

20 ^d *UMR 7194 HNHP (MNHN-CNRS-UPVD), Département Homme et Environnement, Muséum*
21 *National d'Histoire Naturelle, 75013 Paris, France*

22

23 ^e *UMR 7065, IRAMAT, CNRS-Université d'Orleans, Centre Ernest-Babelon, 45071 Orleans,*
24 *France*

25

26 ^f *College of Geographical Sciences, Nanjing Normal University, Nanjing, Jiangsu 210023,*
27 *China*

28

29 ^g *Institute of Culture Heritage, Shandong University, Qingdao Shandong, 266237, China*

30

31 ^h *Institut de Paléontologie Humaine, HNHP CNRS-MNHN, 75013, Paris, France*

32

33 ⁱ *Institute of Archaeology and Ethnography, Siberia Branch, Russian Academy of Sciences,*
34 *Pr. Akademika Lavrentieva 17, Novosibirsk, 630090, Russia*

35

36

37 *Corresponding author.

38 *Email address:* veronique.michel@cnrs.fr (V. Michel).

39 *Full postal address:* Université Côte d'Azur, Pôle Universitaire Saint Jean d'Angély, SJA3,
40 CEPAM, UMR7264, CNRS, UCA, 24 avenue des Diabes Bleus, 06300 Nice, France.

41
42

43

44 **ABSTRACT**

45 Bifacial tools discovered at about a hundred Lower Palaeolithic sites in the Bose Basin,
46 southern China, have been previously dated to around 800,000 years ago. This age was obtained
47 by dating four tektites directly associated with the tools at the Nalai site using the $^{40}\text{Ar}/^{39}\text{Ar}$
48 method (Michel et al., 2021). Similar ages on tektites from the Bogu and Yangwu sites had
49 been previously published, albeit with limited analytical details, by Hou et al. (2000). In this
50 study, a total of eight tektites, discovered alongside abundant lithic artefacts including bifacial
51 tools, were dated with the $^{40}\text{Ar}/^{39}\text{Ar}$ technique, using an incremental temperature increase
52 approach. Six of these tektites are from two Lower Palaeolithic sites in the Bose Basin; three
53 from Xiaomei and three others from Fengshudao (China). The remaining two tektites come
54 from two sites in Vietnam, one from Go Da and the other from Roc-Tung 1. With the exception
55 of the site of Go Da, the tektites were buried in lateritic sediments associated with the stone
56 tools. At the Go Da site, the tektites were found in a layer overlying the deposit containing
57 bifacial tools. The tektites display no signs of fluvial abrasion or reworking, making them
58 potentially strong chronological markers. Chemical analyses of major elements and rare earth
59 elements indicate that the tektites belong to the Australasian tektite group. This is further
60 confirmed by new $^{40}\text{Ar}/^{39}\text{Ar}$ analyses with a weighted mean age of 787.2 ± 8.2 ka (2σ) (MSWD
61 = 0.96, P = 0.45). Therefore, when combined with the available results on Australasian tektites,
62 this suggests a highly precise age of 788.0 ± 2.6 ka (2σ ; P = 0.84) for these tektites and
63 consequently, for the bifacial tools in this part of Southeast Asia, located east of the Movius

64 Line. The presence of bifacial tools attests to either a diffusion of the Acheulean from Africa
65 or a local emergence from previous occupations and traditions in Asia.

66

67 **Keywords:** bifaces, bifacial tools, China, Vietnam, tektite, dating, $^{40}\text{Ar}/^{39}\text{Ar}$, step-heating, Mid-
68 Pleistocene climate transition

69

70 **1. Introduction**

71 Understanding the evolution, diffusion, behavioural changes and adaptation of hominins over
72 time, and the impact and role of climate cycles on the distribution of occupations, is intricately
73 linked to defining an accurate chronological framework. Many questions remain unclear, such
74 as the precise dates of the onset of Lower Palaeolithic-type industries, including the Acheulean,
75 in Asia (arrivals of new populations/traditions or local evolution). The most commonly utilized
76 methods for dating events from the earliest phases of hominin occupations and dispersion, i.e.,
77 2.6-0.6 Ma, are based on radioactive decay (such as K-Ar and its improved derivative $^{40}\text{Ar}/^{39}\text{Ar}$,
78 U-Th, and U-Pb), burial dating by isotopic decay ($^{26}\text{Al}/^{10}\text{Be}$), cumulative processes (Fission
79 track FT, Electron spin resonance ESR, Luminescence), or on the recording of natural processes
80 (such as magnetostratigraphy), often incorporating biochronological data (Pike and Pettitt,
81 2003; Scaillet et al., 2008; Grün et al., 2010; Shen et al., 2012; Tribolo et al., 2013; Jourdan et
82 al., 2014; Lebatard et al., 2014; Hellstrom and Pickering, 2015; Tu et al., 2017; Carbonell et al.,
83 2010; de Lombera-Hermida et al., 2015; Carbonell et al., 2016; Harmand et al., 2015; Semaw
84 et al., 2003; Garcia et al., 2010; Toro-Moyano et al., 2013).

85 In Asia, the earliest evidence, based on current knowledge, was discovered in Central China,
86 and consists of four localities (Xihoudu, Renzidong, Longuppo, Longgudong) potentially
87 indicating the presence of hominins. The ages are between ~2.6 and 1.8 Ma (Shen et al., 2020;
88 Han et al., 2017; Wei et al., 2014; Hou and Zhao, 2010; Li et al., 2017; Bae, 2024, Fig. 1, Fig.

89 [2, Table S1](#)). Several other early sites located in North China date between approximately 2 and
90 1 Ma ago, such as Shangchen, Gongwangling or sites in the Nihewan Formation (Majuangou,
91 Xiantai, Xiaochangliang, Feiliang, Madigou, Cenjiawan, Donggutuo) ([Liu et al., 2014](#); [Zhu et](#)
92 [al., 2004](#); [Zhu et al., 2018](#); [Tu et al., 2017](#); [Ao et al., 2010](#); [Ao et al., 2012](#); [Deng et al., 2006](#);
93 [Keates, 2010](#); [Liu et al., 2013](#); [Zhu et al., 2001, 2003](#); [Yang et al., 2016](#); [Ao et al., 2013](#); [Li et](#)
94 [al., 2016](#); [Pei et al., 2019](#); [Guan et al., 2016](#); [Liu et al., 2013](#); [Wang et al., 2005](#); [Yang et al.,](#)
95 [2017](#); [Yang et al., 2020](#), see [Table S1 for details](#)). All these sites have yielded lithic
96 assemblages, described by some as crudely-made tools. Recent dating studies have improved
97 the chronological framework of early hominin presence in this part of Eurasia, as described in
98 [Appendix A \(Table S1, Fig. 2\)](#).

99 The emergence and diffusion of the Acheulean (with new technological features including
100 Large Cutting Tools-LCTs) is still enigmatic. The earliest evidence is located in Africa, with
101 sites corresponding to the transition from the Oldowan/Mode 1 (core-and-flake industries) to
102 the Early Acheulean/Mode 2. This occurred diachronically around 1.95-1.0 Ma ([Lepre et al.,](#)
103 [2011](#); [Beyene et al., 2013](#); [Mussi et al., 2023a](#)). These African industries evolved over time into
104 what is described as the Classical Acheulean from ~1.5 to 0.8 Ma ([Mussi et al., 2023b](#); [Galloti](#)
105 [and Mussi, 2017](#)). Outside Africa, the Acheulean is younger, with evidence in the Levant of an
106 early “Out of Africa” dispersion for this tradition at ~1.6-1.4 Ma at Ubeidiya ([Martinez-Navarro](#)
107 [et al., 2012](#); [Sagi, 2005](#); [Rink et al., 2007](#)), possibly followed by a second wave at ~800 ka at
108 Gesher Benot Yakov ([Goren-Inbar et al., 2018](#)), suggesting, at the least recurrent phases of
109 diffusion outside Africa.

110 Moving to Asia, two hypotheses have been put forward regarding the emergence of the
111 Acheulean culture beyond the “Movius Line” in an area where LCTs were considered to be
112 absent ([Movius, 1948](#); [Bae, 2024](#)): either this represents the diffusion of the Acheulean from

113 Africa, as observed in the Near East, or it is a local emergence from previous occupations and
114 traditions in Asia (Bae, 2024).

115 It is therefore essential to accurately date sites with LCTs (bifaces/bifacial tools/handaxes
116 according to studies and authors) in Eurasia in order to contribute to discussions on the onset
117 of this/these new traditions(s) in Asia, and to better define the possible diffusion of what is
118 described in Africa as the Acheulean. Only we then will gain insights into Pleistocene hominin
119 mobility and behavioural strategies in response to a continually changing climate (Bae et al.,
120 2018, Larick and Ciochon, 2015; Qin and Sun, 2023). For convenience, throughout our paper,
121 we use the generic terminology of LCTs to designate lithic assemblages with bifaces, handaxes
122 and bifacial tools.

123 In Michel et al. (2021), tektites in close association with LCTs at the Nalai site (Bose Basin,
124 South China) were dated to 809 ± 12 ka from 55 total fusion subsamples. A probability density
125 distribution yielded an age centred at 797 ± 6 ka, tentatively suggesting that they might be part
126 of the Australasian tektite strewnfield recently dated to 788 ± 3 ka (2σ , $P = 0.54$) by the
127 $^{40}\text{Ar}/^{39}\text{Ar}$ method (Jourdan et al., 2019). In this new study, our aim is to improve the accuracy
128 of our preliminary dating result of the Bose sites (Michel et al., 2021) and obtain new dates for
129 two sites in Central Vietnam yielding LCTs. We dated tektites *via* $^{40}\text{Ar}/^{39}\text{Ar}$ analysis by the
130 “step-heating” method in order to circumvent inherited argon present in tektites during the
131 initial steps. Furthermore, with this approach, inverse isochron ages can be calculated, which
132 resolves and takes into account any inherited $^{40}\text{Ar}^*$ present in the samples in the calculation,
133 provided that its argon isotopic composition is homogenous, thus leading to more accurate
134 results (Jourdan et al., 2019). $^{40}\text{Ar}/^{39}\text{Ar}$ dating analyses were conducted on tektites from two
135 archaeological sites located in the Bose Basin in China and from two others sites located in
136 Vietnam (An Khê): Xiaomei, Fengshudao, Go Da and Roc Tung 1, respectively (Fig. 1, Fig.

137 [S1, Fig. S2](#)). Major and trace element geochemistry was applied to tektites to assess whether
138 they were part of the Australasian strewnfield.

139

140 **2. Australasian tektites: origin, background chronology and chronological markers**

141 Tektites are glasses produced by the melting of the continental crust during the impact of a
142 meteorite. This impact causing the formation of Australasian tektites is supposed to have
143 resulted in the formation of a crater located in Indochina, or more likely, in southern Laos.
144 According to the recent study by [Sieh et al. \(2020\)](#), the crater would be buried under the Bolaven
145 volcanic field, near the northern limit of the strewnfield ([Fig. 1](#)), although firm evidence is still
146 lacking. These tektites have been found at varying distances from the impact structure, spanning
147 regions from Southeast Asia to Antarctica, with a chemical composition characteristic of the
148 group of Australasian tektites ([Koeberl, 1990](#); [Heide et al., 2001](#); [Glass and Koeberl, 2006](#);
149 [Schwarcz et al., 2016](#)).

150 Tektites closely associated with artefacts from the Bose Basin in China were initially dated
151 using fission track dating ([Guo et al., 1997](#)). The authors obtained an age of 732 ± 39 ka for the
152 tektites of the Bogu site ([Fig. S1](#)). Subsequently, the $^{40}\text{Ar}/^{39}\text{Ar}$ method was applied to two
153 tektites from the Bogu site and one from the Yangwu site, but these results were published
154 without age spectra or detailed analytical data ([Hou et al., 2000](#)) ([Fig. S1](#)). The authors obtained
155 an overall weighted mean age of 803 ± 6 ka (2σ) from the isochron ages of three samples ([Hou](#)
156 [et al., 2000](#); [Potts et al., 2000](#)).

157 This first $^{40}\text{Ar}/^{39}\text{Ar}$ dating of tektite in Bose Palaeolithic sites, presented by [Hou et al. \(2000\)](#)
158 was questioned by [Koeberl and Glass \(2000\)](#). The latter authors cast doubt on the association
159 of tektites with the artefacts and claimed that tektites are generally found in deposits younger
160 than their isotopic age. They thus called for caution in using them as stratigraphic markers
161 ([Koeberl and Glass, 2000](#); [Keates, 2000](#)). [Potts et al. \(2000\)](#) responded clearly, affirming that

162 the Bose tektites are *in situ* and associated with the stone tools in terrace T4, as described by
163 [Hou et al. \(2000\)](#), in the same way as the stone tools found alongside tektites at the Gaolingpo
164 site ([Xie et al., 2021](#)). They attributed the tektite age to the tools as there is no geomorphological
165 and stratigraphical indication of the redeposition of either the tools or tektites ([Potts et al.,](#)
166 [2000](#)). Later, [Wang et al. \(2014\)](#) presented a detailed morphological study of the Fengshudao
167 site and its bifacial industry. In this site, the first excavated association of tektites, dating to ca.
168 803 ka, with LCTs (including bifaces), and found *in situ*, was described in one stratigraphic
169 level in terrace T4, indicating that the Bose Basin handaxes most likely date to the Early to
170 Middle Pleistocene transition ([Fig. 2](#)). However, according to [Langbroek \(2015\)](#), the age of the
171 earliest bifaces in China and the close association between tektites and bifaces have not yet
172 been demonstrated, although this was clearly established by [Wang and Bae \(2015\)](#), and later
173 confirmed at the Nalai site with Australasian tektites and bifaces found together *in situ* ([Michel](#)
174 [et al., 2021](#)). It is important to note that two Australasian tektites found *in situ* at the Sangiran
175 area have been successfully used as chronological markers. They are consistent with the
176 magnetic polarity stratigraphy and predate the Matuyama-Brunhes transition (MB) ([Hyodo et](#)
177 [al., 2011](#)). The data demonstrate the near co-occurrence of the tektite level and the
178 magnetostratigraphic constraint, arguing that the last occurrence of Sangiran hominins dates to
179 ~ 0.79 Ma ([Fig. 2](#)).

180 Later, [Jourdan et al. \(2019\)](#) conducted precise dating on four Australasian tektites from Western
181 Australia, Thailand, Vietnam, and southern China, including a tektite from the Bose Basin
182 previously dated by [Hou et al. \(2000\)](#). The exact origin of the tektite from the Bose Basin was
183 not specified by [Jourdan et al. \(2019\)](#). Age plateau and isochron diagrams yielded concordant
184 data with a weighted-mean age of 788.1 ± 2.8 (P = 0.54) for these Australasian tektites, which
185 aligns closely with the less precise $^{40}\text{Ar}/^{39}\text{Ar}$ age of 793 ± 14 ka published by [Schwarz et al.](#)
186 [\(2016\)](#).

187 3. Xiaomei and Fengshudao sites in Southern China: Geography, stratigraphy and lithic 188 assemblages

189 The history of Palaeolithic research in the Bose Basin has been thoroughly documented by
190 Wang et al. (2014). Approximately a hundred sites have been discovered in this basin (de
191 Lumley et al., 2020; Wang et al., 2024). In these three abovementioned studies, the
192 geography/geology of the Bose Basin with its Quaternary terrace stratigraphy (see Fig. S3, Fig.
193 S4), as well as overviews of the site's location and lithic assemblages, are also described in
194 detail.

195 The Xiaomei site is located in Xiaomei village, Youjiang district, Bose city, Guangxi Zhuang
196 Autonomous Region (23°46'41.5" N, 106°42'21.9" E), on the fourth terrace of the Youjiang
197 River (Fig. S1, Fig. S3, Fig. S4, Fig. S5). It was discovered in the 1980s during an
198 archaeological survey covering an area of 350,000 m². Many lithic artefacts and a few tektites
199 were exposed on the ground surface of the laterite deposits at the site. The lithic series were
200 made up of diversified LCTs, including pick and tongue-shaped bifaces typical of the area (Fig.
201 3, n° 6), on sandstone or quartzite pebbles (Fig. 3, n° 7 and 8), associated with flake-tools
202 (scrapers), and notably a large unifacial core on a massive thick quartzite pebble (Fig. 3, n° 9)
203 with centripetal removals. A test excavation conducted in 1996 unearthed artefacts, associated
204 with tektites. Based on geomorphology and artefacts, the age of this site is assumed to be the
205 same as that of Bogu site.

206 The Fengshudao site (23°57'39''N, 106°40'39''E) is situated along the south bank of the
207 Chengbihe River, a significant tributary of the Youjiang River (Fig. S1, Fig. S3, Fig. S4). The
208 site is located in the fourth terrace, spanning 100 metres from east to west, with a sloping terrain
209 from north to south of approximately 10 to 30 metres. Discovered in 2004, the site was
210 excavated from 2004 to 2005, revealing nearly 100 artefacts and nine tektites *in situ* from an
211 excavated area of 62.6 m² (Wang et al., 2014). The lithic assemblage at the Fengshudao site

212 includes the same diversity as at Xiaomei (Fig. 3, n° 5) with in addition, evidence of the use of
213 bipolar debitage. The main raw materials consist of sandstone, quartzite and quartz collected
214 as pebbles. Both tektites and LCTs are found in exactly the same layer within the laterite (Wang
215 et al., 2024) (Fig. 4).

216 The bifaces exhibit the characteristic shape of the Bose Basin bifaces (Hou et al., 2000; Xie
217 and Bodin, 2007; Zhang et al., 2010; Huang et al., 2012; Wang et al., 2014; Feng et al. 2018;
218 Wang et al., 2024). They are notably short, broad and stocky, featuring a tongue-shaped
219 extremity (Fig. 3, n° 1, 2 and 3).

220

221 **4. Go Da and Roc Tung 1 sites in Central Vietnam: Geography, stratigraphy and lithic** 222 **assemblage**

223 Following the discovery of sites with LCTs near the city of An Khê in Central Vietnam in 2014,
224 by Vietnamese archaeologists, systematic excavations have been conducted since 2015
225 (Derevianko et al., 2018) (Fig. 1, Fig. S2).

226 Several other similar Palaeolithic sites were identified at the Roc Tung location, situated on the
227 left bank of the Ba River. Artefacts were collected on the surface or discovered *in situ* during
228 excavations and test pits, with similar stratigraphic contexts. The Roc Tung 1 site (14°02'253"
229 N; 108°40'822" E) is situated on a high and relatively flat area of agricultural land. The
230 stratigraphy is well-documented through excavations and various test pits (Derevianko et al.,
231 2018). Three layers have been identified below the surface debris of an irrigation canal. The
232 cultural layer, situated at the top of the laterite (Layer 3), has yielded several *in situ* artefacts
233 associated with tektites (Fig. S6, Fig. 5).

234 Go Da (13°58'306" N; 108°39'136" E; 440 m a.s.l.) is located downstream, near An Khê, on a
235 sloping hill, 900 m west of the Ba River (Fig. S2). The stratigraphy established during the
236 excavation is somewhat different on this right bank of the Ba (Derevianko et al. (2018);

237 [Kandyba et al. \(2021\)](#) ([Fig. S7](#)). The stratigraphic sequence begins with a substantial weathering
238 crust (layer 1) of the granite bedrock, succeeded by slope wash sediments (layer 2). The cultural
239 horizon at Go Da formed during these erosion and slope wash processes, probably in a cooler
240 climate than the present one. Archaeological materials are specifically situated at the top of the
241 weathering crust and at the base of the slope wash layer ([Fig. S7](#)). Tektites found in the upper
242 part of this layer 2 indicate that hominins were present at Go Da before the deposition of
243 Australasian tektites. In other words, it can be asserted that the industries at Go Da predate those
244 at Roc Tung 1, where artefacts are found *in situ* with tektites.

245 The local industry is well described by [Derevianko et al. \(2018\)](#) and [Kandyba et al. \(2021\)](#). The
246 lithic assemblage from the Roc Tung 1 site, collected on the surface but also in stratigraphy
247 context during excavations and test pits, includes over 126 pieces ([Derevianko et al. 2018](#)),
248 made on pebbles or boulders. This lithic industry from the left bank of the Ba River is made on
249 local raw materials, most often quartzite cobbles or blocks, but also other raw materials of lesser
250 quality, such as vein quartz. Many tested pebbles have been identified in the assemblage, no
251 doubt corresponding to knappers' efforts to select good-quality blanks ([Fig. 6](#)).

252 As in the other An Khê-tradition assemblages ([Derevianko et al. 2018](#)), the main features of the
253 industry at Roc Tung 1 are heavy-duty-tools including numerous LCTs (bifaces, picks),
254 choppers, and chopping-tools ([Fig. 6, n° 2 and 3](#)) and light-duty tools, such as scrapers and
255 pointed tools, often made on flakes. Finally, flakes and cores attest to simple reduction
256 processes: cores mainly bear a single debitage surface with unipolar or centripetal removals and
257 a limited prepared or cortical striking platform.

258 The lithic assemblage at the Go Da site comprises around a hundred artefacts ([Derevianko et](#)
259 [al. 2018; Kandyba et al 2021](#)), comparable to those from Roc Tung 1. These consist of
260 numerous split tested pebbles, often large in size, hammerstones on rounded granite pebbles, a
261 heavy-duty tool kit with mainly thick, short and stocky LCTs (including bifaces and picks), on

262 quartzite pebbles or slabs. Some display a tongue-shaped extremity. Others are choppers on
263 long and massive quartzite pebbles, and pointed tools and scrapers (Fig. 6, n°1). The cores,
264 flakes and small flakes indicate *in situ* reduction processes, mainly unifacial and unipolar
265 removals. This assemblage displays all the characteristics of the An Khê industry, as well as
266 regional traditions.

267 These two assemblages from Roc Tung 1 and Go Da share many similarities to industries from
268 the Bose Basin in China, notably those from Fengshudao and Xiaomei, discussed in this study.

269

270 **5. Materials and methods**

271 5.1. Materials.

272 Our analysed tektites come from the Fengshudao and Xiaomei sites (Bose Basin, China),
273 and Roc Tung 1 and Go Da sites (Central Vietnam). They were discovered *in situ* associated
274 with tools (including LCTs), except for the Go Da site, where the tektites were found in a layer
275 overlying bifacial tool-bearing deposits, providing a minimum age for the artefacts.

276 Three tektites (F1, F2, F3) collected from the laterite layer of terrace T4 at the Fengshudao
277 site (Fig. 7), display a very thin profile (~0.4-0.6 g) and show no signs of fluvial abrasion. They
278 are very angular and sharp, suggesting that no river re-depositing occurred. Additionally, three
279 tektites, namely B1 (10.2 g), B2 (8.7 g), and B3 (6.5 g), were excavated from the same laterite
280 layer from terrace T4 at the Xiaomei site, with a rounder morphology than the others (Fig. 7).

281 Two tektites from Central Vietnam; one larger tektite, GD (19.1 g), excavated at the Go Da
282 site, and another, large and very angular tektite, RT1 (10.3 g), with no signs of fluvial abrasion,
283 excavated at the Roc Tung 1 site, complete the sample. The GD tektite is rounder, similar to
284 the Xiaomei tektites studied here, but neither show signs of fluvial abrasion or reworking.

285 5.2. Method

286 Before analysis, the eight tektite samples were cleaned in an ultrasonic water bath to remove
287 surface-bonded residues (Fig. 7). The thinner tektites (F1, F2, F3) were reduced to pieces. For
288 the larger ones (B1, B2, B3, GD, and RT1), a piece of each tektite was extracted from the
289 original tektites and reduced to pieces. Some were further crushed in an agate mortar and
290 divided into subsamples for multiple analyses. For $^{40}\text{Ar}/^{39}\text{Ar}$ dating, subsamples 400-500 μm
291 in size, from F1, F2, B1, B2, B3, GD and RT1 tektites, were cleaned with an HNO_3 2N
292 ultrasonic bath for 15 minutes, in HF 2% for 20 minutes, in H_2O , and then in acetone.
293 Subsamples weighing 30-70 mg were analysed using the "step-heating" method with
294 incremental temperature increases to produce an age spectrum and inverse isochron. The
295 $^{40}\text{Ar}/^{39}\text{Ar}$ analyses were conducted at the Western Australian Argon Isotope Facility (Australia)
296 using an ARGUS VI multicollection instrument and following the procedure described by
297 Jourdan et al. (2019), used for dating the Australasian tektites. The raw data (Appendix B) were
298 processed using the ArArCALC software (Koppers, 2002) and the ages were calculated using
299 the FCs standards (Jourdan and Renne, 2007), for which an age of 28.294 Ma ($\pm 0.13\%$) was
300 used (Renne et al., 2011), along with the decay constants recommended by Renne et al. (2011).
301 Our criteria for plateau determination are as follows: plateaus must include at least 70% of ^{39}Ar .
302 The plateau should be distributed over a minimum of three consecutive steps agreeing at 95%
303 confidence level and satisfying a probability of fit (P) of at least 0.05. Plateau ages are given at
304 the 2σ level and are calculated using the mean of all the plateau steps, each weighted by the
305 inverse variance of their individual analytical error. Uncertainties include analytical and J-value
306 errors. Errors with all sources of uncertainties such as the decay constants errors increase the
307 uncertainty by ± 0.2 ka for those samples and are indicated by a square bracket (e.g., [± 3 ka]).
308 The composition of major and trace elements presented in Tables S2 and S3, was determined
309 for all tektites by Laser Ablation Inductively Coupled Plasma Mass Spectrometry at the Centre
310 Ernest-Babelon of the IRAMAT (CNRS/Orléans University) or by Inductively Coupled Plasma

311 Optical Emission Spectrometry at SARM (Service d'Analyses des Roches et des Minéraux,
312 CRPG Nancy, France (see additional details in SI). The composition of major elements of
313 tektites N411, N425, N862, N959 from Nalai site in the Bose Basin, China, as reported by
314 Michel et al. (2021), was supplemented with the analysis of rare earth elements and is presented
315 in Table S3.

316

317 6. Results

318 6.1 Chemical composition

319 The major elemental compositions obtained for the tektites B1, B2, B3 (Xiaomei), F1, F2, F3
320 (Fengshudao), GD (Go Da) and RT1 (Roc Tung 1), are presented in Table S2. They comprise
321 the following ranges: 70.05-74.74 % for SiO₂, 11.13-15.44 % for Al₂O₃, 4.17-4.96 % for FeO,
322 1.77-2.67 % for CaO, 2.06-2.42 % for K₂O, 1.92-2.67 % for MgO, 0.93-1.51 % for Na₂O, 0.68-
323 0.78 % for TiO₂, 0.08-0.10 % for MnO, 0.03-0.07 % for P₂O₅. These values are very close to
324 those of the tektites from Nalai (N411, N425, N862, N959) (Michel et al., 2021) (Table S2). In
325 Figure 8, these values are compared with various groups of tektites according to Schwarz et al.
326 (2016) and Wesgate et al. (2021). Figure 8 shows that our tektites belong to the group of
327 Australasian tektites. Tektites from Vietnam (GD and RT1) are very slightly different to those
328 from the Bose Basin. They belong to the subgroup of indochinite showing some regional
329 compositional variation in comparison with the australite subgroup, but ultimately belong to
330 the same Australasian group. In the same way as the Australasian tektites, our tektites exhibit
331 light rare-earth-element-(REE)-enriched compositions with a marked negative EU anomaly, as
332 described by Koeberl (1990), Son and Koeberl (2005), Amare and Koeberl (2006), Wesgate et
333 al. (2021) and Schwarz et al. (2016) (Fig. 9).

334

335 6.2 ⁴⁰Ar/³⁹Ar dating

336 We obtained seven plateau ages ranging from 779 ± 19 ka (MSWD = 0.53; P=0.93) to $827 \pm$
337 57 ka (MSWD = 0.09; P = 1.00) and including between 91 and 100 % of the total released ^{39}Ar
338 (Fig. 10, Appendix B). Inverse isochrons yielded similar ages ranging from 774 ± 24 to $842 \pm$
339 67 and with trapped $^{40}\text{Ar}/^{36}\text{Ar}$ ratios in error of the atmospheric value of 298.6 ± 0.3 and ranging
340 from 293.3 ± 4.9 to 300.8 ± 6.0 (Appendix C). The K/Ca ratio (derived from $^{39}\text{Ar}_K/^{37}\text{Ar}_{Ca}$)
341 shows homogenous values across a given tektite but varies among samples with average values
342 ranging from 0.32 ± 0.18 to 1.29 ± 0.11 . The seven plateau ages (P = 0.84) and inverse isochron
343 ages (P = 0.25) are all indistinguishable from each other, indicating the dating of a single event,
344 as expected for tektites originating from a single impact. Furthermore, all intercept $^{40}\text{Ar}/^{36}\text{Ar}$
345 values define a single population (P = 0.57) with a weighted mean of 296 ± 3 , suggesting that
346 no inherited $^{40}\text{Ar}^*$ is present in the samples analysed in this study. Therefore, we calculated a
347 single weighted mean age of 787.2 ± 8.2 ka (2σ ; MSWD = 0.96; P = 0.45) as the best estimate
348 for the impact event that produced these tektites. This age is indistinguishable from the previous
349 age of 788.1 ± 2.8 (Jourdan et al., 2019), indicating that the tektites are part of the Australasian
350 strewnfield, as also evidenced by their chemical composition. When combined with our new
351 age, we obtained a conclusive best age estimate of 788.0 ± 2.6 [2.8] ka (2σ ; P = 0.84) for the
352 Australasian tektites that will be used in the rest of this study.

353

354 **7. Discussion on the new results of the Chinese and Vietnamese sites regarding the** 355 **emergence and diffusion of the Acheulean in Eurasia**

356 *7.1 Emergence of the Acheulean in Africa and its initial diffusion*

357 The emergence of the Acheulean in Africa is dated to around 1.75 to < 1.0 Ma (i.e., in southern
358 Ethiopia, Beyene et al., 2013) and around 1.76 Ma years ago at Kokiselei 4 in Kenya (Lepre et
359 al., 2011) but may have occurred earlier, around 1.95 Ma years ago at Garba IV (Upper Awash,
360 Ethiopia, Mussi et al., 2023a). This shift was characterized among others (flaking methods,

361 land-use patterns) by hominin capability to produce large flakes and LCTs, including for
362 example, handaxes, picks and sometimes cleavers. The earliest LCTs (including bifaces),
363 outside Africa are reported at ~1.4-1.2 Ma ago in Ubeidiya in the Levant (Martinez-Navarro et
364 al., 2012; Sagi, 2005; Rink et al., 2007), and are also dated to ~1.5 Ma in Attirampakkam, India,
365 indicating a rapid diffusion throughout Eurasia, if we consider that these industries are related
366 to the African Acheulean. These types of LCTs are not present, earlier than 0.9-0.7 Ma in
367 Western Europe (Pappu et al., 2011; Vallverdu et al., 2014; Voinchet et al., 2015; Antoine et
368 al., 2019; Moncel et al., 2020a; Moncel et al., 2020b). In Asia, the core-and-flake series (Mode
369 1) persist when Lower Palaeolithic/Acheulean (Mode 2) industries with LCTs (bifaces/bifacial
370 tools/handaxes) appear in some areas around 1.5-0.8 Ma ago. The number of discovered sites
371 increase during the Mid-Pleistocene climate transition (MPT) (1.0-0.6 Ma) suggesting that this
372 period played a crucial role in the diffusion of hominins in Eurasia (Fig. 2, Table S1).

373

374 7.2. New insights from Chinese and Vietnamese sites

375 These new assemblages with LCTs in Asia are currently found in four main Chinese areas
376 (specifically Dingcun, Bose Basin, Luonan Basin, and the Danjiangkou Reservoir Region
377 DRR) (Li et al., 2018, Li et al., 2014). Unfortunately, dating details are limited, except for the
378 site of Yunxian (open-air site of Xuetangliangzi, DRR region, Central China), where two *Homo*
379 *erectus* crania were discovered with one handaxe and 13 LCTs collected from the surface (Li
380 et al., 2018). This site is approximately dated between ~1.1-0.85 Ma using both
381 paleomagnetism, biochronology and ESR dating on teeth and quartz (de Lumley and Li, 2008;
382 Echassoux et al., 2008; Tissoux et al., 2008; Feng, 2008) (Fig.1, Fig.2, Table S1). Many other
383 sites with LCTs, up to 200 LCTs, were discovered in this area but further chronological research
384 is required. They are regarded as the most significant persistence of LCTs for a long period,
385 from the late Early Pleistocene to the early part of the Late Pleistocene (Li et al., 2018).

386 Our results on four Chinese and Vietnamese sites provide strong and accurate data on Asian
387 human occupations with LCTs dated to ~ 788 ka. Through these new data, we contribute to
388 understanding of the chronology and diffusion of the earliest populations in Asia.

389 Early human populations thrived and expanded across mainland East Asia, from low latitudes
390 whatever their technology (e.g., the Bose Basin) to high northern latitudes (e.g., the Nihewan
391 Basin, Zhoukoudian). The associated industry is often roughly dated using paleomagnetism, as
392 seen in Maliang (Nihewan Formation, North China), Wutaicun (Central China), Longgangsi-2
393 and 3 (Central China). The determined ages are approximately ~0.78 Ma (Wang et al., 2005),
394 ~0.9 Ma and ~1.2-0.7 Ma (Sun et al., 2017) respectively. Despite approximate dating, an
395 overview of paleoenvironmental and archaeological data in the Nihewan Basin reveals changes
396 in hominin presence and indicates that sustained occupation in high latitudes characterized by
397 strong seasonality was not possible until the Late Pleistocene, as evidenced by chronological
398 gaps (Yang et al., 2020). Mode1/Oldowan industries persisted in Asia at Bailong Cave with
399 human teeth in Central China, dated between ~0.78 Ma and ~0.51 Ma, and also using multi-
400 dating methods such as paleomagnetism, $^{26}\text{Al}/^{10}\text{Be}$ burial on quartz and ESR/U-series on teeth
401 (Liu et al., 2015; Han et al., 2018; Kong et al., 2018).

402 Moving outside China, this lithic industry is also evidenced at the site of Kalinga between
403 around 1.05 and 0.63 Ma, in the Philippines (Ingicco et al., 2018), and between around 1.01
404 and 0.7 Ma at Mata Menge and Wolo Sege in Indonesia (Brumm et al., 2016). During the same
405 period, an Acheulean-type industry is present at Shuigou-Huixinggou, in Central China, but
406 approximatively dated to ~0.9 Ma by paleomagnetism (Li et al., 2017). Other Mode 1/Mode 2
407 sites dated by alternative radioisotopic methods provide more precise dating (Fig.2, Table S1).

408 This is the case for Zhoukoudian Locality 1, in North China, where human remains and
409 industries with bifacial tools and flake-tools (Derevianko, 2008) are well dated to ~0.78-0.4 Ma

410 using multi-dating methods, such as paleomagnetism, $^{26}\text{Al}/^{10}\text{Be}$ burial and U-Th (Shen et al.,
411 2009, Shen et al., 2016).

412 Li et al. (2018) propose that the technological transmission hypothesis could be a suitable
413 explanation for the emergence of Chinese LCTs technology and suggest a diffusion of the
414 Acheulean-type tradition by hominins from west to east to China and other Asia areas as
415 Vietnam. Other authors propose a local onset derived from previous Mode 1/core-and-flake
416 assemblages (convergence), giving rise to the An Khê tradition observed at the Go Da and Roc
417 Tung Lower Palaeolithic sites in Vietnam (Derevianko et al., 2018) and the Acheulean in the
418 Bose Lower Palaeolithic sites (Wang et al., 2014; Wang and Bae, 2015; Wang et al., 2024; Bae,
419 2024) (Fig.1, Fig.2, Table S1).

420 Our results highlight that the industries at the Bose and An Khê sites are now well dated to
421 788.0 ± 2.6 ka (2σ) by dating *in situ* Australasian tektites associated with the bifaces. This
422 significant chronological marker accurately positions the industries at the Bose and An Khê
423 sites within the chronological sequence of industries in Asia and also indicates a well-
424 established presence of LCTs and possibly the Acheulean-type tradition in this region of Asia.

425

426 **8. Conclusion**

427 Our dating of Australasian tektites discovered *in situ* alongside artefacts at the Bose sites in
428 southern China and An Khê in Central Vietnam using $^{40}\text{Ar}/^{39}\text{Ar}$ gives an age of 788.0 ± 2.6
429 [2.8] ka. This age indicates that LCTs (including bifaces), and thus what can be described as
430 the Acheulean, developed in this part of Asia around 788 ka during the Mid-Pleistocene climate
431 transition, regardless of the hypothesis regarding the onset of the Acheulean (Fig. 2, Table S1).

432 Our result can be compared to the age of the Acheulean industry also found at around 1.1-0.8
433 Ma at DRR sites, Yunxian and Shuigou-Huixinggou in Central China. This new LCT-making
434 tradition is penecontemporaneous with persistent core-and-flake series (Mode 1) at Nihewan in

435 northern China, at Bailong, as well as Longgangsi in Central China. This persistence of
436 assemblages without LCTs extends to the Philippines at Kalinga and Indonesia at Mata Menge
437 and Wolo Sege, with for some, the presence of *Homo erectus* while the Acheulean-type
438 assemblages persist at Zhoukoudian (~0.8-0.6 Ma) in North China. The Bose and An Khê sites
439 can be considered as the earliest well-dated evidence of Acheulean-type tradition beyond the
440 Movius Line in eastern Asia, showing that hominins in these areas were capable of making
441 LCTs, including bifaces at ~788 ka.

442

443 **Acknowledgements**

444 This work was carried out with partial financial support from CEPAM-CNRS. Louise Byrne is
445 acknowledged for English improvements of the manuscript. The Handling Editor, Christopher
446 J. Bae, and the two anonymous reviewers are thanked for their constructive comments and
447 helpful suggestions for improving this manuscript.

448

449 **Figure captions**

450 **Figure 1.** Portion of the Australasian tektite strewnfield (modified from [Wesgate et al., 2021](#))
451 with a potential crater impact in southern Laos ([Sieh et al., 2020](#)). The Movius Line is
452 represented by the red dashed line, separating Western Asia, where LCTs were discovered from
453 Eastern Asia, where LCTs, were considered absent ([Movius, 1948](#)). However, since then,
454 Acheulean assemblages with LCTs have been discovered east of the line ([Bae, 2024](#)). The
455 archaeological sites are located south of the 45°N parallel and are classified in chronological
456 order. The sites are dated using methods such as radiometric dating and/or relative dating,
457 including biochronology and paleomagnetism, based on current knowledge ([Table S1](#)). The
458 distribution indicates sites with Mode 1 (core-and-flake assemblages) (marked with stars), those

459 with *Homo* remains (marked with circles), and those associated with Acheulean/Mode 2
460 (marked with triangles). Red symbols represent the studied sites, while black symbols denote
461 other key sites (see details in **Tab S1**): (1) Masol, India, (2) Riwat, Pakistan, (3) Attirampakkam,
462 India, (4) Renzidong, Central China, (5) Xihoudu, northern China (6) Longgupo, Central China,
463 (7) Longgudong, Central China, (8) Shangchen, Central China, (9) Gongwangling (Lantian
464 man), North China, (10) Niujuanbao, Southwest China, (11) Many sites in the Nihewan Basin,
465 northern China: e.g. Donggutuo, Maliang, Feilang Xiaochangliang, Xiantai, Majuangou,
466 Madigou, Cenjiawan Xiaochangliang, (12) Sangiran, Bapang, Lower Lahar unit, Central Java,
467 Indonesia, (13) Longgangsi 3-2, (14) Soa Basin, Ola Bula Formation, Mata Menge, Wolo Sege,
468 Central Flores, eastern Indonesia (15) Yunxian, DRR sites, Central China, (16) Wutaicun,
469 Central China, (17) Shuigou-Huiximggou, Central China, (18) Meipu, Central China, (19)
470 Trinil, Java, Indonesia, (20) Many sites in the Bose Basin, Bogu, Yangwu; Nalai, Fengshudao,
471 Xiaomei (this study), (21) Roc Tung 1 and Go Da, Central Vietnam (this study), (22) Kalinga,
472 Philippines, (23) Bailong, Central China, (24) Zhoukoudian Locality 1, northern China, (25)
473 Yiyuan, northern China.

474

475 **Figure 2.** Chronological sequence of Palaeolithic sites with hominin fossils and/or lithic
476 assemblages according to geographical location and correlation with marine isotope stages and
477 $\delta^{18}\text{O}$ stacks (Lisiecki and Raymo, 2005). The horizontal grey band denotes the Mid-Pleistocene
478 climate transition MPT (1.0-0.6 Ma).

479

480 **Figure 3.** Lithic artefacts from Fengshudao site (1 to 5) and from Xiaomei site (6 to 9). 1 to 3-
481 tongue-shaped bifaces (N007612; N007622; N007623); 4- chopper (N007775); 5- large flake
482 (N007566); 6-tongue-shaped biface (N73 H05); 7 & 8- picks (N94 5.6; N193 G2); 9- large core
483 (N59).

484

485 **Figure 4.** Fengshudao site excavation. Photographs showing the *in situ* discovery of biface No.
486 Z007773 (2) in the laterite layer, in close association with tektite No. FSD-059 (1).

487

488 **Figure 5.** Roc Tung 1 excavation. Photograph showing an *in situ* discovery of a pebble core
489 No 16.RT1.ST79 (2) in the laterite layer (Layer 3), in close association with a tektite No 14 (1).
490 Bifaces were excavated in the same layer.

491

492 **Figure 6.** Lithic artefacts from Go Da site (1) and from Roc Tung 1 site (2 and 3). 1- scraper;
493 2- chopper; 3- biface.

494

495 **Figure 7.** Photograph of tektites analysed in this study: F1, F2, F3 (~0.4-0.6 g) are three thin
496 tektites excavated from Fengshudao site, Bose Basin, China; B1 (10.2 g), B2 (8.7 g), B3 (6.5
497 g) are three tektites excavated from Xiaomei site, Bose Basin, China ; GD (19.1 g) is a tektite
498 excavated from Go Da site and RT1 (10.3 g) is a tektite excavated from Roc Tung 1 site,
499 Vietnam. GD and RT1 were cleaned with a H₂O ultrasonic bath.

500

501 **Figure 8.** Chemical composition of various tektite groups, based on the original figure by
502 [Schwarz et al. \(2016\)](#) with modifications. This figure includes a comparison of compositions
503 with cited references by [Schwarcz et al. \(2016\)](#) ([Taylor, 1962](#); [Chapman and Schreiber, 1969](#);
504 [O'Reilly et al., 1983](#); [Koeberl et al., 1997](#); [Meisel et al., 1997](#); [Albin et al., 2000](#); [Son and](#)
505 [Koeberl, 2005](#); [Amare and Koeberl, 2006](#)), including Belize (BZ1) (Central America, with
506 impact glasses formed at 804 ± 9 ka, [Rochette et al., 2021](#)), Ivory Coast tektite (Ivorite), and

507 Australasian tektites such as Indochinite B (Muong-Nong), Western Canada (WC1) with
508 impact glasses formed at 785 ± 7 ka ($^{40}\text{Ar}/^{39}\text{Ar}$ age, [Schwarcz et al., 2016](#)), and those with a
509 weighted FT age of 822 ± 20 ka from Malaysia, Java, Australia (group A) ([Wesgate et al.,](#)
510 [2021](#)). Additionally, we present the chemical compositions of tektites from Nalai, Xiaomei,
511 Fengshudao, Roc Tung 1 and Go Da sites, demonstrating similarities to the Australasian tektite
512 group.

513

514 **Figure 9.** Rare earth element abundances for tektites N411, N425, N862, N959 (Nalai site); F1,
515 F2, F3: tektites (Fengshudao site); B1, B2, B3 (Xiaomei site); GD (Go Da site); RT1 (Roc Tung
516 1 site). They are chondrite-normalized rare-earth-element (REE) abundance curves (chondrite
517 concentrations are from [McDonough and Sun, 1995](#)). The abundances are compared with
518 various tektites, including Belize (BZ1), Ivory Coast tektite 1, and Australasian tektites, such
519 as Indochinite B (Muong-Nong), Western Canada (WC1) ([Schwarcz et al., 2016](#)), and those
520 from Malaysia (UT1389), Java (UT2336), Australia (UT2330, UT2334, UT1392, UT2402)
521 ([Wesgate et al., 2021](#)). The patterns of our tektites are similar to Australasian tektites ([Schwarcz](#)
522 [et al., 2016](#); [Wesgate et al., 2021](#)), but distinct to the Belize and the Ivory coast tektites with
523 their lower concentrations and different impact events ([Schwarcz et al., 2016](#)).

524

525 **Figure 10.** $^{40}\text{Ar}/^{39}\text{Ar}$ age spectra of tektites. Plateau age given at the 2σ level. B1, B2, B3:
526 tektites from Xioamei site; F1, F2: tektites from Fengshudao site; RT1: tektite from Roc Tung
527 1; GD: tektite from Go Da.

528

529 **Appendix A.** Supplementary information.

530 **MC2.** Ar isotopic data corrected for blank.

531 **MC3.** $^{39}\text{Ar}/^{40}\text{Ar}$ vs. $^{36}\text{Ar}/^{40}\text{Ar}$ inverse isochron plots.

532 **MC4. Tables S2 and S3**

533 **References**

- 534 Albin, E. F., Norman, M. D., Rodan, M., 2000. Major and trace element compositions of
535 georgiites: clues to the source of North American tektites. *Meteoritic Planetary Science* 35,
536 795–806.
537
- 538 Amare, K., Koeberl, C., 2006. Variation of chemical composition in Australasian tektites from
539 different localities in Vietnam. *Meteoritic & Planetary Science* 41, 107–123.
540
- 541 Ao, H., Deng, C., Dekkers, M.J., Liu, Q., Qin, L., Xiao, G., Chang, H., 2010. Astronomical
542 dating of the Xiantai, Donggutuo and Maliang Paleolithic sites in the Nihewan Basin (North
543 China) and implications for early human evolution in East Asia. *Palaeogeography,*
544 *Palaeoclimatology, Palaeoecology* 297, 129-137.
- 545 Ao, H., An, Z.S., Dekkers, M.J., Wei, Q., Pei, S.W., Zhao, H., Zhao, H.L., Xiao, G.Q., Qiang,
546 X.K., Wu, D.C., Chang, H., 2012. High-resolution record of geomagnetic excursions in the
547 Matuyama chron constrains the ages of the Feiliang and Lanpo Paleolithic sites in the Nihewan
548 Basin, North China. *Geochemistry, Geophysics, Geosystems* 13, Q08017.
- 549 Ao, H., An, Z., Zhisheng, A., Dekkers, M.J., Li, Y., Xiao, G., Zhao, H., Qiang, X., 2013.
550 Pleistocene magnetochronology of the fauna and Paleolithic sites in the Nihewan Basin:
551 Significance for environmental and hominin evolution in North China. *Quaternary*
552 *Geochronology* 18, 78-92.
553
- 554 Antoine P., Moncel M-H., Locht J-L. Bahain J-J., Voinchet P., Herisson D., Hurel A., 2019.
555 The earliest record of Acheulean human occupation in North-West Europe. *Nature Scientific*
556 *Reports* 9, 13091.
557 <https://doi.org/10.1038/s41598-019-49400-w>
558
- 559 Bae, C.J., 2024. *The Paleoanthropology of Eastern Asia*, University of Hawai'i Press,
560 Honolulu.
561
- 562 Bae, C.J., Li, F., Cheng, L., Wang, W., Hong, H., 2018. Hominin distribution and density
563 patterns in Pleistocene China: Climatic influences. *Palaeogeography, Palaeoclimatology,*
564 *Palaeoecology* 512, 118-131.
565
- 566 Beyene, Y., Katoh, S., WoldeGabriel, G., Hart, W.K., Uto, K., Sudo, M., Kondo, M., Hyodo,
567 M., Renne, P.R., Suwa, G., Asfaw, B., 2013. The characteristics and chronology of the earliest
568 Acheulean at Konso, Ethiopia. *PNAS* 110, 1584-1591.
569
- 570 Brumm, A., van den Bergh, G., Storey, M., Kurniawan, I., Alloway, B.V., Setiawan, R.,
571 Setiyabudi, E., Grün, R., Moore, M.W., Yurnaldi, D., Puspaningrum, M.R., Wibowo, U.P.,
572 Insani, H., Sutisna, I., Westgate, J.A., Pearce, N.J.G., Duval, M., Meijer, H.J.M., Aziz, F.,
573 Sutikna, T., van der Kaars, S., Morwood, M.J., 2016. Age and context of the oldest known
574 hominin fossils from Flores. *Nature* 534, 249–253.
575

576 Carbonell, E., Sala Ramos, R., Rodriguez, X.P., Mosquera, M., Ollé, A., Vergès J.M., Martinez-
577 Navarro, B., Bermudez de Castro, J.M., 2010. Early hominid dispersals: A technological
578 hypothesis for « out of Africa ». *Quaternary International* 223-224, 36-44.
579

580 Carbonell, E., Barsky, D., Sala, R., Celiberti, V., 2016. Structural continuity and technological
581 change in Lower Pleistocene toolkits. *Quaternary International* 393, 6-18.
582

583 Chapman, D.R., Scheiber, L.C., 1969. Chemical Investigation of Australasian Tektites. *Journal*
584 *of Geophysical Research* 74, 6737-6776.
585

586 Deng, C.L., Wei, Q., Zhu, R.X., Wang, H.Q., Zhang, R., Ao, H., Chang, L., Pan, Y.X., 2006.
587 Magnetostratigraphic age of the Xiantai Paleolithic site in the Nihewan Basin and implications
588 for early human colonization of Northeast Asia. *Earth Planet. Sci. Lett.* 244, 336–348.
589

590 Derevianko, A.P., 2008. Paleoenvironment. The Stone Age. The Bifacial technique on China.
591 *Archaeology, Ethnology & Anthropology of Eurasia* 33/1, 2-32.

592 Derevianko, A.P., Kandyda, A.V., Khac Su, N., Gladyshev, S.A., Gia Doi, N., Lebedev, V.A.,
593 Chekha, A.M., Rybalko, A.G., Kharevich, V.M., Tsybankov, A.A., 2018. The Discovery of a
594 Bifacial Industry in Vietnam. *Archaeology, Ethnology and Anthropology of Eurasia* 46/3, 3-21.
595

596 Echassoux, A., Moigne, A.-M., Moullé, P.-E., Li, T., Feng, X.B., Li, W., WU, Z.,
597 Fauquembergue, E., Magnaldi, B., 2008. Les faunes de grands mammifères du site de l’Homme
598 de Yunxian. In : de Lumley H., Li T. (Eds.), *Le site de l’Homme de Yunxian*. CNRS éditions,
599 Paris, pp. 253-364.
600

601 Feng, X., 2008. Stratégie de débitage et mode de façonnage des industries du Paléolithique
602 inférieur en Chine et en Europe entre 1 Ma et 400 000 ans. Ressemblances et différences de la
603 culture de l’homme de Yunxian et Acheuléen européen. *L’Anthropologie* 112, 423-447.
604

605 Feng, X., Qi, Y., Li, Q., Ma, X., Liu, K., 2018. The industry of the Lower Paleolithic site of
606 Baigu, Bose Basin, Guangxi Zhuang autonome Province, PR China. *L’Anthropologie* 122, 14–
607 32.
608

609 Gallotti, R., & Mussi, M., 2017. Two Acheuleans, two humankinds. From 1.5 to 0.85 Ma at
610 Melka Kunture (Upper Awash, Ethiopian highlands). *Journal of Anthropological Sciences* 95,
611 137-181.
612

613 Garcia, T., Féraud, G., Falguères, C., de Lumley, H., Perrenoud, C., Lordkipanidze, D., 2010.
614 Earliest human remains in Eurasia: New ⁴⁰Ar/³⁹Ar dating of the Dmanisi hominid-bearing
615 levels, Georgia. *Quaternary Geochronology* 5, 443-451.
616

617 Glass, B.P., Koeberl, C., 2006. Australasian microtektites and associated impact ejecta in the
618 South China Sea and the Middle Pleistocene supereruption of Toba. *Meteoritics & Planetary*
619 *Science* 41, 305-326.
620

621 Goren-Inbar, N. Alperson-Alif, N., Sharon, G., Herzlinger, G., 2018. The Acheulian site of
622 Geshen Benot Ya ‘aqov. Volume IV. The lithic Assemblages. Springer, Cham.
623

624 Grün, R., Aubert, M., Hellstrom, J., Duval, M., 2010. The challenge of direct dating old human
625 fossils. *Quaternary International* 223-224, 87-93.
626

627 Guan, Y., Wang, F-G, Xie, F., Pei, S-W, Zhou, Z-Y, Gao, X., 2016. Flint knapping strategies
628 at Cenjiawan, an Early Paleolithic site in the Nihewan Basin, North China. *Quaternary*
629 *International* 400, 86-92.
630

631 Guo, S.-L., Huang, W., Hao, X.-H., Chen, B.L., 1997. Fission Track Dating of Ancient Man
632 Site in Baise, China, and its significances in space research, Paleomagnetism and Stratigraphy.
633 *Radiation Measurements* 28, 565-570.
634

635 Han, F., Bahain, J.-J., Deng, C., Boëda, E., Hou, Y., Wei, G., Huang, W., Garcia, T., Shao, Q.,
636 He, C., Falguères, C., Voinchet, P., Yin, G., 2017. The earliest evidence of hominid settlement
637 in China: Combined electron spin resonance and uranium series (ESR/U-series) dating of
638 mammalian fossil teeth from Longgupo cave. *Quaternary International* 434, 75-83.
639

640 Han, F., Shao, Q., Bahain, J.-J., Sun, X., Yin, G., 2018. Coupled ESR and U-series dating of
641 Middle Pleistocene hominin site Bailongdong cave, China, *Quaternary Geochronology* 49, 291-
642 296.
643
644

645 Harmand, S., Lewis, J.E., Feibel, C.S., Lepre, C.J., Prat, S., Lenoble, A., Boës, X., Quinn, R.,
646 Brenet, M., Arroyo, A., Taylor, N., Clément, S., Daver, G., Brugal, J.-P., Leakey, L. Mortlocks,
647 R.A., Wright, J.D., Lokorodi, S., Kirwa, C., Kent, D.V., Roche, H., 2015. 3.3-million-year-old
648 stone tools from Lomekwi 3, West Turkana, Kenya. *Nature* 521, 310-315.
649

650 Heide, K., Heide, G., Kloess, G., 2001. Glass chemistry of tektites. *Planet. Space Sci.* 49, 839–
651 844.
652

653 Hellstrom, J., Pickering, R., 2015. Recent advances and future prospects of the U-Th and U-Pb
654 chronometers applicable to archaeology. *Journal of Archaeological Science* 56, 32-40.
655

656 Hou, Y., Potts, R., Baoyin, Y., Zhengtang, G., Deino, A., Wie, W., Clark, J., Guangmao, X.,
657 Weiwen, H., 2000. Mid-Pleistocene Acheulean-like Stone Technology of the Bose Basin, South
658 China. *Science* 287, 1622–1626.
659

660 Hou, Y.M., Zhao, L.X., 2010. An archaeological view for the presence of early humans in
661 China. *Quaternary International* 223-224, 10-19.
662

663 Huang, S., Wang, W., Bae, C. J., Xu, G., Liu, K., 2012. Recent Paleolithic field investigations
664 in Bose Basin (Guangxi, China). *Quaternary International* 281, 5–9.
665

666 Hyodo, M., Matsu'ura, S., Kamishima, Y., Kondo, M., Takeshita, Y., Kitaba, I., Danhara, T.,
667 Aziz, F., Kurniawan, I., Kumai, H., 2011. High-resolution record of the Matuyama-Brunhes
668 transition constrains the age of Javanese *Homo erectus* in the Sangiran dome, Indonesia. *PNAS*
669 108, 19563-19568.
670

671 Ingicco, T., van den Bergh, G.D., Jago-on, C., Bahain, J.-J., Chacon, M.G., Amano, N.,
672 Forestier, H., King, C., Manalo, K., Nomade, S., Pereira, A., Reyes, M.C., Sémah, A.-M., Shao,
673 Q., Voinchet, P., Falguères, C., Albers, P.C.H., Lising, M., Lyras, G., Yurnaldi, D., Rochette,

674 P., Baustita, A., de Vos, J., 2018. Earliest known hominin activity in the Philippines by 709
675 thousand years ago. *Nature* 557, 233-237.

676

677 Jourdan, F., Renne, P.R., 2007. Age calibration of the Fish Canyon sanidine $^{40}\text{Ar}/^{39}\text{Ar}$ dating
678 standard using primary K-Ar standards. *Geochimica et Cosmochimica Acta* 71, 387-402.

679

680 Jourdan, F., Mark, D.F., Vérati, C. (eds), 2014. *Advances in $^{40}\text{Ar}/^{39}\text{Ar}$ dating: from
681 archaeological to planetary sciences-introduction*. Geological Society, London, Special
682 Publications 378, 1–8.

683

684 Jourdan, F., Nomade, S., Wingate, M.T.D., Eroglu, E., Deino, A., 2019. Ultraprecise age and
685 formation temperature of the Australasian tektites constrained by $^{40}\text{Ar}/^{39}\text{Ar}$ analyses.
686 *Meteoritics & Planetary Science* 54, 2373-2591.

687

688 Kandyba, A.V., Chekha, A.M., Doi, N.G., Su, N. K., Gladyshev, S.A., Derevianko, A.P., 2021.
689 The early Paleolithic Go Da site and the Bifacial lithic industries of Southeast Asia.
690 *Archaeology, Ethnology & Anthropology of Eurasia* 49, 3-14.

691

692 Keates, S.G., 2000. Tektites and the age paradox in Mid-Pleistocene China. *Science* 289, 507a.

693

694 Keates, S.G., 2010. Evidence for the earliest Pleistocene hominid activity in the Nihewan Basin
695 of northern China. *Quaternary International* 223-224, 408-417.

696

697 Koeberl, C., 1990. The geochemistry of tektites: An overview. *Tectonophysics* 171, 405–422.

698

699 Koeberl C., Bottomley R., Glass B.P., Storzer D., 1997. Geochemistry and age of Ivory Coast
700 tektites and microtektites. *Geochimica et Cosmochimica Acta* 61, 1745-1772.

701

702 Koeberl, C., Glass, B.P., 2000. Tektites and the age paradox in Mid-Pleistocene China. *Science*
703 289, 507a.

704

705 Kong, Y., Deng, C., Liu, W., Pei, S., Sun, L., Ge, J., Yi, L., Zhu, R., 2018. Magnetostratigraphic
706 dating of the hominin occupation of Bailong Cave, central China. *Scientific Reports* 8, 9699.

707

708 Koppers, A.A.P., 2002. ArArCALC-software for $^{40}\text{Ar}/^{39}\text{Ar}$ age calculations. *Computers &
709 Geosciences* 28, 605–619.

710

711 Langbroek, M., 2015. Do tektites really date the bifaces from the Bose (Baise) Basin, Guangxi,
712 southern China?. *Journal of Human Evolution* 80, 175-178.

713

714 Larick, R., Ciochon, R.L., 2015. Early hominin Biogeography in Island Southeast Asia.
715 *Evolutionary Anthropology* 24, 185-213.

716

717 Lebatard, A.-E., Alçiçek, M.C., Rochette, P., Khatib, S., Vialet, A., Bouldes, N., Bourlès, D.J.,
718 Demory, F., Guipert, G., Mayda, S., Titov, V.V., Vidal, L., de Lumley, H., 2014. Dating the
719 *Homo erectus* bearing travertine from Kocabaş (Denizli, Turkey) at at least 1.1 Ma. *Earth and
720 Planetary Science Letters* 390, 8-18.

721

722 Lepre, C.J., Roche, H., Kent, D.V., Harmand, S., Quinn, R.L., Brugal, J.-P., Texier, P.-J.,
723 Lenoble, A., Feigél, C.S., 2011. An earlier origin for the Acheulian. *Nature* 477, 81-85

724 Li, H., Li, C., Kuman, K., 2014. Rethinking the “Acheulean” in East Asia: Evidence from recent
725 investigations in the Danjiangkou Reservoir Region, central China. *Quaternary International*
726 347, 163-175.
727

728 Li, H., Li, C., Kuman, K., 2017. Longgudong, an Early Pleistocene site in Jianshi, South China,
729 with stratigraphic association of human teeth and lithics. *Science China Earth Sciences* 60, 452-
730 462.
731

732 Li, H., Kuman, K., Li, C., 2018. What is currently (un)known about the Chinese Acheulean,
733 with implications for hypotheses on the earlier dispersal of hominids. *C.R. Palevol* 17, 120-
734 130.
735

736 Li, X., Pei, S., Jia, Z., Guan, Y., Niu, D., Ao, H., 2016. Paleoenvironmental conditions at
737 Madigou (MDG), a newly discovered Early Paleolithic site in the Nihewan Basin, North China.
738 *Quaternary International* 400, 100-110.
739

740 Li, X., Ao, H., Dekkers, M.J., Roberts, A.P., Zhang, P., Lin, S., Huang, W., Hou, Y., Zhang,
741 W., An, Z., 2017. Early Pleistocene occurrence of Acheulian technology in North China.
742 *Quaternary Science Reviews* 156, 12-22.
743

744 Lisiecki, L.E., Raymo, M.E., 2005. A Pleistocene-Pleistocene stack of 57 globally distributed
745 benthic $\delta^{18}\text{O}$ records. *Paleoceanography and Paleoclimatology* 20, PA1003.
746

747 Liu, Y., Hu, Y., Wei, Q., 2013. Early to Late Pleistocene human settlements and the evolution
748 of lithic technology in the Nihewan Basin, North China: A macroscopic perspective.
749 *Quaternary International* 295, 204-214.
750

751 Liu, C.-R., Yin, G.-M., Deng, C.-L., Han, F., Song, W.-J., 2014. ESR dating of the Majuangou
752 and Banshan Paleolithic sites in the Nihewan Basin, North China. *Journal of Human Evolution*
753 73, 58-63.
754

755 Liu, Y., Hu, Y., Wei, Q., 2013. Early to Late Pleistocene human settlements and the evolution
756 of lithic technology in the Nihewan Basin, North China: A macroscopic perspective.
757 *Quaternary International* 295, 204-214.
758

759 Liu, X., Shen, G., Tu, H., Lu, C., Granger, D.E., 2015. Initial $^{26}\text{Al}/^{10}\text{Be}$ burial dating of the
760 hominin site Bailong Cave in Hubei Province, central China. *Quaternary International* 389, 235-
761 240.
762

763 Lombera-Hermida de, A., Bargallo, A., Terradillos-Bernal, M., Huguet, R., Vallverdu, J.,
764 Garcia-Anton, M.-D., Mosquera, M., Ollé, A., Sala, R., Carbonell, E., Rodriguez-Alvarez, X.-
765 P., 2015. The lithic industry of Sima del Elefante (Atapuerca, Burgos, Spain) in the context of
766 Early and Middle Pleistocene technology in Europe. *Journal of Human Evolution* 82, 95-106.
767

768 Lumley de, H., Li, T., (Eds.), 2008. *Le site de l’homme de Yunxian : Quyanhekou, Quingqu,*
769 *Yunxian, Province de Hubei.* CNRS Editions, Paris.
770

771 Lumley de, H., Cauche, D., Pollet, G., Notter, O., Rossini-Notter, E., Xie, G., Lin, Q, Feng, X.,
772 Ghen, X., Qi, Y., Wei, J., Wang, W., Huang, Q., 2020. Les industries lithiques du Paléolithique

773 ancien du bassin de Bose. Province autonome du Guangxi Zhuang, Chine du Sud. CNRS
774 Editions, Paris, 325 p. ISBN: 978-2-271-13406-6
775

776 Matinez-Navarro, B., Belmaker, M., Bar-Yosef, O., 2012. The Bovid assemblage (Bovidae,
777 Mammalia) from the Early Pleistocene site of 'Ubeidiya, Israel: Biochronological and
778 paleoecological implications for the fossil and lithic bearing strata. *Quaternary International*
779 267, 78-97.
780

781 McDonough, W. F., Sun, S.-S., 1995. The composition of the Earth. *Chemical Geology* 120,
782 223-253.
783

784 Meisel, T., Lange, J.-M., Krähenbühl, U., 1997. The chemical variation of moldavite tektites:
785 simple mixing of terrestrial sediments. *Meteoritics Planetary Science* 32, 493–502.
786

787 Michel, V., Feng, X., Shen, G., Cauche, D., Moncel, M.-H., Gallet, S., Gratuze, B., Wei, J.,
788 Ma, X., Liu, K., 2021. First $^{40}\text{Ar}/^{39}\text{Ar}$ analyses of Australasian tektites in close association with
789 bifacially worked artifacts at Nalai site in Bose Basin, South China: The question of the early
790 Chinese Acheulean. *Journal of Human Evolution*, 153, 102953.
791

792 Moncel, M-H., Santagata, C., Pereira, A., Nomade, S., Voinchet, P., Bahain, J-J., Daujeard, C.,
793 Curci, A. Lemorini, C., Hardy, B., Eramo, G., Berto, C., Raynal, J-P., Arzarello, M., Mecozzi,
794 B., Iannucci, A., Sardella, R., Allegretta, I., Delluniversità, E., Terzano, R., Dugas, P., Jouanic,
795 G., Queffelec, A., d'Andrea, A., Valentini, R., Minucci, E., Carpentiero, L., Piperno, M.,
796 2020a. The origin of early Acheulean expansion in Europe 700 ka ago: new findings at
797 Notarchirico (Italy). *Nature. Scientific Reports* 10(1), 1-16.
798 <https://doi.org/10.1038/s41598-020-68617-8>
799

800 Moncel M-H., Despriée J., Courcimaut G., Voinchet P., Bahain J-J., 2020b. La Noira site
801 (Centre, France) and the technological behaviours and skills of the earliest Acheulean in
802 Western Europe between 700 and 600 kyrs. *Journal of Paleolithic Archeology* 3 (3), 255-301.
803 <https://doi.org/10.1007/s41982-020-00049-2>
804

805 Movius, H., 1948. The Lower Palaeolithic Cultures of Southern and Eastern Asia. *Transactions*
806 *of the American Philosophical Society* 38, 329-420.
807

808 Mussi, M., Skinner, M.M., Melis, R.T., Pneras, J., Rubio-Jara, S., Davies, T.W., Geraads, D.,
809 Bocherens, H., Briatico, G., Le Cabec, A., Hublin, J.-J., Gidna, A., Bonnefille, R., Di Bianco,
810 L., Mendez-Quinta, E., 2023a. Early *Homo erectus* lived at high altitudes and produced both
811 Oldowan and Acheulean tools. *Science* 382, 713-718.
812

813 Mussi, M., Altamura, F., Di Bianco, L., Bonnefille, R., Gaudzinski-Windheuser, S., Geraads,
814 D., Melis, R.T., Panera, J., Piarulli, F., Pioli, L., Ruta, G., Sanchez-Dehesa Galn, S., Mendez -
815 Quintas, E. 2023b. After the emergence of the Acheulean at Melka Kunture (Upper Awash,
816 Ethiopia): From Gombore IB (1.6 Ma) to Gombore Iy (1.4 Ma), Gombore iδ (1.3 Ma) and
817 Gombore II OAM test pit C (1.2 Ma). *Quaternary International* 657, 3-25.
818

819 O'Reilly, T.C., Haskin, L.A., King, E.A., 1983. Element correlations among north American
820 tektites. *14th Luna Planet. Sci.*, 580-581 (abstract).
821

822 Pappu, S., Gunnell, Y., Akhilesh, K., Braucher, R., Taieb, M., Demory, F., Thouveny, N., 2011.
823 Early Pleistocene Presence of Acheulian Hominins in South India. *Science* 331, 1596-1599.
824

825 Pei, S., Deng, C., de la Torre, I., Jia, Z., Ma, D., Li, X., Wang, X., 2019. Magnetostratigraphic
826 and archaeological records at the Early Pleistocene site complex of Madigou (Nihewan Basin):
827 Implications for human adaptations in North China. *Palaeogeography, Palaeoclimatology,*
828 *Palaeoecology* 530, 176-189.
829

830 Pike, A.W.G., Pettitt, P.B., 2003. U-series Dating and Human Evolution. In *Uranium Series*
831 *Geochemistry* (edited by B. Bourdon, G.M. Henderson, C.C. Lundstrom, et al.). *Reviews in*
832 *Mineralogy and Geochemistry* 52, 607-630.
833

834 Potts, R., Huang, W., Hou, Y., Deino, A., Baoyin, Y., Zhengtang, G., Clark, J., 2000. Tektites
835 and the age paradox in Mid-Pleistocene China. *Response. Science* 289, 507a.
836

837 Qin, Z., Sun, X., 2023. Glacial-Interglacial Cycles and Early Human Evolution in China. *Land*
838 12, 1683.
839

840 Renne, P.R., Balco, G., Ludwig, K.R., Mundil, R., Min, K., 2011. Response to the comment by
841 W.H. Schwarz et al. on "Joint determination of K-40 decay constants and Ar-40*/K-40 for the
842 Fish Canyon sanidine standard, and improved accuracy for Ar-40/Ar-39 geochronology" by PR
843 Renne et al. (2010). *Geochimica et Cosmochimica Acta* 75, 5097-5100.
844

845 Rink, W.J., Bartoll, J., Schwarcz, H.P., Shane, P., Bar-Osef, O., 2007. Testing the reliability of
846 ESR dating of optically exposed buried quartz sediments. *Radiation Measurements* 42, 1618-
847 1626.
848

849 Rochette, P., Beck, P., Bizzarro, M., Braucher, R., Cornec, J., Debaille, V., Devouard, B.,
850 Gattacceca, J., Jourdan, F., Moustard, F., Moynier, F., Nomade, S., Reynard, B., 2021. Impact
851 glasses from Belize represent tektites from the Pleistocene Pantasma impact crater in
852 Nicaragua. *Communications earth & environment* 2, 94.
853

854 Sagi, A., 2005. Magnetostratigraphy of 'Ubeidiya Formation, Northern Dead Sea Transform,
855 Israel. M.S. Dissertation, The Hebrew University.
856

857 Scaillet, S., Vita-Scaillet, G., Guillou, H., 2008. Oldest human footprints dated by Ar/Ar. *Earth*
858 *and Planetary Science Letters* 275, 320–325.
859

860 Schwarz, W.H., Trieloff, M., Bollinger, K., Gantert, N., Fernandes, V.A., Meyer, H.-P.,
861 Povenmire, H., Jessberger, E.K., Guglielmino, M., Koeberl, C., 2016. Coeval ages of
862 Australasian, Central American and Western Canadian tektites reveal multiple impacts 790 ka
863 ago. *Geochimica et Cosmochimica Acta* 178, 307-319.
864

865 Semaw, S., Rogers, M.J., Quade, J., Renne, P.R., Butler, R.F., Dominguez-Rodrigo, M., Stout,
866 D., Hart, W.S., Pickering, T., Simpson, S.W., 2003. 2.6-Million-year-old stone tools and
867 associated bones from OGS-6 and OGS-7, Gona, Afar, Ethiopia. *Journal of Human Evolution*
868 45, 169-177.
869

870 Shen, C., Zhang, X., Gao, X., 2016. Zhoukoudian in transition: Research history, lithic
871 technologies, and transformation of Chinese Palaeolithic archaeology. *Quaternary International*
872 400, 4-13.

873

874 Shen, G.J., Gao, X., Gao, B., Granger, D.E., 2009. Age of Zhoukoudian *Homo erectus*
875 determined with $^{26}\text{Al}/^{10}\text{Be}$ burial dating. *Nature* 458, 198-200.

876

877 Shen, G.J., Michel, V., Despriée, J., Han, F., Granger, D., 2012. Datation d'enfouissement par
878 $^{26}\text{Al}/^{10}\text{Be}$ et son application préliminaire à des sites du Paléolithique inférieur en Chine et en
879 France. *L'Anthropologie* 116, 1-11.

880

881 Shen, G., Wang, Y., Tu, Hua, Tong, H., Wu, Z., Kuman, K., Fink, D., Granger, D.E., 2020.
882 Isochron $^{26}\text{Al}/^{10}\text{Be}$ burial dating of Xiboudu: Evidence for the earliest human settlement in
883 northern China. *L'Anthropologie* 124, 102790.

884

885 Sieh, K., Herrin, J., Jicha, B., Angel, D.S., Moore, J.D.P., Banerjee, P., Wiwegwin, W.,
886 Sihavong, V., Singer, B., Chualaowanich, T., Charusiri, P., 2020. Australasian impact crater
887 buried under the Bolaven volcanic field, Southern Laos. *PNAS* 117, 1346-1353.

888

889 Son, T.H., Koeberl, C., 2005. Chemical variation within fragments of Australasian tektites.
890 *Meteoritics & Planetary Science* 40, 805-815.

891

892 Sun, X., Lu, H., Wang, S., Yi, L., Li, Y., Bahain, J.-J., Vionchet, P., Hu, X., Zeng L., Zhang,
893 W., Zhuo, H., 2017. Early human settlements in the southern Qinling Mountains, central China,
894 *Quaternary Science Reviews* 164, 168-186.

895

896 Taylor, S.R., 1962. The chemical composition of australites. *Geochimica et Cosmochimica*
897 *Acta* 26, 685-722.

898

899 Tissoux, H., Bahain, J.-J., de Lumley, H., Li, T., Feng, X., Li, W., 2008. Essai de datation par
900 les méthodes combinées (RPE/U-Th) de dents d'herbivores et par RPE de quartz blanchis
901 extraits des sédiments fluviaux provenant du site de l'Homme de Yunxian. In : de Lumley H.,
902 Li T. (Eds.), *Le site de l'Homme de Yunxian*. CNRS éditions, Paris, pp. 237-252.

903

904 Toro-Moyano, I., Martinez-Navarro, B., Augusti, J., Souday, C., Bermudez de Castro, J.M.,
905 Martinon-Torres, M., Fajardo, B., Duval, M., Falguères, C., Oms, O., Pares, J.M., Andon, P.,
906 Julia, R., Garcia-Aguilar, J.M., Moigne, A.-M., Espigares, M.P., Ros-Montoya, S., Palmqvist,
907 P., 2013. The oldest human fossil in Europe, from Orce (Spain). *Journal of Human Evolution*
908 65, 1-9.

909

910 Tribolo, C., Mercier, N., Douville, E., Joron, J.-L., Reyss, J.-L., Rufer, D., Cantin, N., Lefrais,
911 Y., Miller, C.E., Porraz, G., Parlington, J., Rigaud, J.-P., Texier, P.-J., 2013. OSL and TL dating
912 of the Middle Stone Age sequence at Diepkloof Rock Shelter (South Africa): A clarification.
913 *Journal of Archaeological Science* 40, 3401-3411.

914

915 Tu, H., Shen, G., Granger, D., Yang, X., Lai, Z., 2017. Isochron $^{26}\text{Al}/^{10}\text{Be}$ burial dating of the
916 Lantian hominin site at Gongwangling in Northwestern China. *Quaternary Geochronology* 41,
917 174-179.

918

919 Vallverdu, J., Saladié, P., S., Rosas, A., Huguet R., Caceres, I., Mosquera, M., Garcia-Taberno,
920 A., Estalrich, A., Lozana-Fernandez, I., Pineda-Alcala, A., Carrancho, A., Villalain, J.J.,
921 Bourlès, D., Braucher R., Lebatard, E., Vilalta, J., Esteban-Nadal, M., Bennisar M.L., Bastir,
922 M., Lopez-Polin L., Ollé, A., Vergés, J.M., Ros-Montoya, S., Martinez-Navarro, B., Garcia,
923 A., Martinell, J., Exposito, I., Burjachs, F., Agusti, J., Carbonell, E., 2014. Age and Date for
924 Early Arrival of the Acheulian in Europe (Barranc de la Boella, la Canonja, Spain). *PLoS One*
925 9, e103634.
926

927 Voinchet, P., Moreno, D., Bahain, J-J., Tissoux, H., Tombret, O., Falguères, Moncel, M-H. C.,
928 Schreve, D., Candy, I., Antoine, P., Ashton, N., Beamish, M., Cliquet, D., Despriée, J., Lewis,
929 S., Limondin-Lozouet, N., Locht, J-L., Parfitt, S., Pope, M., 2015. New chronological data
930 (ESR and ESR/U-series) for the earliest Acheulean sites of north-western Europe. *J. Quat. Sci.*
931 30, 610–622.
932

933 Wang, H., Deng, C., Zhu, R., Wei, Q., Hou, Y., Boëda, E., 2005. Magnetostratigraphic dating
934 of the Donggutuo and Maliang Paleolithic sites in the Nihewan Basin, North China. *Quaternary*
935 *Research* 64, 1-11.
936

937 Wang, W., Bae, C.J., Huang, S., Huang, X., Tian, F., Mo, J., Huang, Z., Huang, C., Xie, S., Li,
938 D., 2014. Middle Pleistocene bifaces from Fengshudao (Bose Basin, Guangxi, China). *Journal*
939 *of Human Evolution* 69, 110-122.
940

941 Wang, W., Bae, C.J., 2015. How old are the Bose (Baise) Basin (Guangxi, southern China)
942 bifaces? The Australasian tektites question revisited. *Journal of Human Evolution* 80, 171-174.
943

944 Wang, W., Fan, Y., Bae, C., 2024. The Bose (South China) Handaxes: Early Palaeolithic
945 Bifaces and Early Hominin Cognition. In: *The Oxford Handbook of Cognitive Archaeology*
946 (eds. K.A. Overmann, F.L. Coolidge), chap. 31, p. 741-770.
947

948 Wei, G., Huang, W., Chen, S., He, C., Pang, L., Wu, Y., 2014. Paleolithic culture of Longgupo
949 and its creators. *Quaternary International* 354, 154-161.
950

951 Wesgate, J.A., Pillans, B.J., Alloway, B.V., Pearce, N.J.G., Simmonds P., 2021. New fission-
952 track ages of Australasian tektites define two age groups: discriminating between formation and
953 reset ages. *Quaternary Geochronology* 66, 101113.
954

955 Xie, G.-M., Bodin, E., 2007. Les industries paléolithiques du Bassin de Bose (Chine du Sud).
956 *L'Anthropologie* 111, 182–206.
957

958 Xie, G., Chen, X., Li, D., Yu, M., Hu, Z., Lu, H., Huang, Q., Lin, Q., 2021. Stratigraphy and
959 chronology of the palaeolithic industry in Bose Basin, South China: Excavation of Gaolingpo.
960 *Archaeological Research in Asia* 26, 100284.
961

962 Yang, S.-X., Hou, Y.-M., Yue, J.-P., Petraglia, M.D., Deng, C.-L., Zhu, R.-X., 2016. The Lithic
963 Assemblages of Xiaochangliang, Nihewan Basin: Implications for Early Pleistocene Hominin
964 Behaviour in North China. *PLoS ONE* 11(5), e0155793.
965

966 Yang, S.-X., Petraglia, M.D., Hou, Y.-M., Yue, J.-P., Deng, C.-L., Zhu, R.-X., 2017. The lithic
967 assemblages of Donggutuo, Nihewan basin: Knapping skills of Early Pleistocene hominins in
968 North China. *PLoS ONE* 12, e0185101.

969

970 Yang, S.-X., Deng, C.-L., Zhu, R.-X., Petraglia, M.D., 2020. The Paleolithic in the Nihewan
971 Basin, China: Evolutionary history of an Early to Late Pleistocene record in Eastern Asia.
972 *Evolutionary Anthropology* 29, 125-142.

973

974 Zhang, P., Huang, W., Wang, W., 2010. Acheulean handaxes from Fengshudao, Bose sites of
975 South China. *Quaternary International* 223–224, 440–443.

976

977 Zhu, R.X., Hoffman, K.A., Potts, R., Deng, C.L., Pan, Y.X., Guo, B., Shi, C.D., Guo, Z.T.,
978 Yuan, B.Y., Hou, Y.M., Huang, W.W., 2001. Earliest presence of humans in northeast Asia.
979 *Nature* 413, 413–417.

980

981 Zhu, R., An, Z., Potts, R., Hoffman, K.A., 2003. Magnetostratigraphic dating of early humans
982 in China. *Earth-Science Reviews* 61, 341-359.

983

984 Zhu, R.X., Potts, R., Xie, F., Hoffmn, K.A., Deng, C.L., Shi, C.D., Pan, Y.X., Wang, H.Q., Shi,
985 R.P., Wang, Y.C., Shi, G.H., Wu, N.Q., 2004. New evidence on the earliest human presence at
986 high northern latitudes in northeast Asia. *Nature* 431, 559-562.

987

988 Zhu, Z., Dennell, R., Huang, W., Wu, Y., Qiu, S., Yang, S., Rao, Z., Hou, Y., Xie, J., Han, J.,
989 Ouyang, T., 2018. Hominin occupation of the Chinese Loess Plateau since about 2.1 million
990 years ago. *Nature* 559, 608-612.

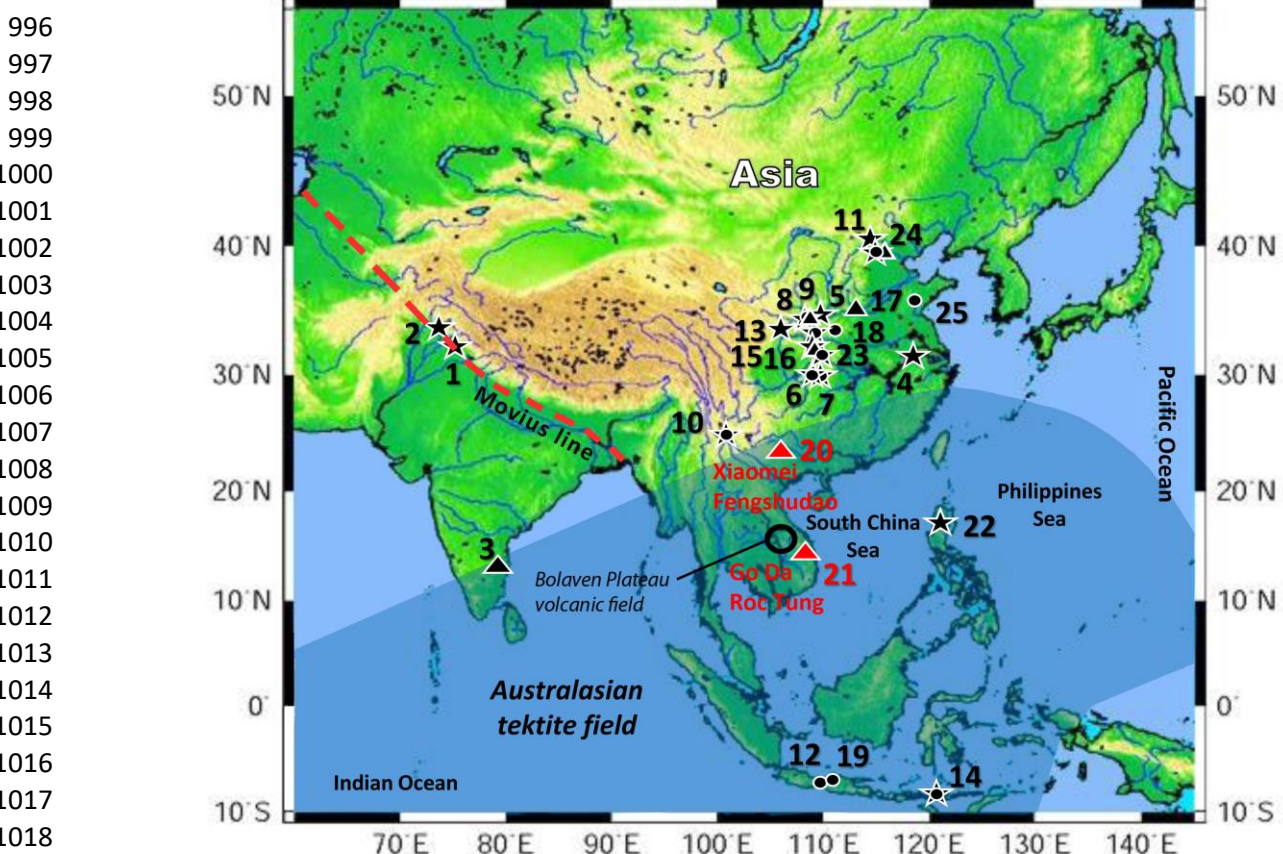
991

992

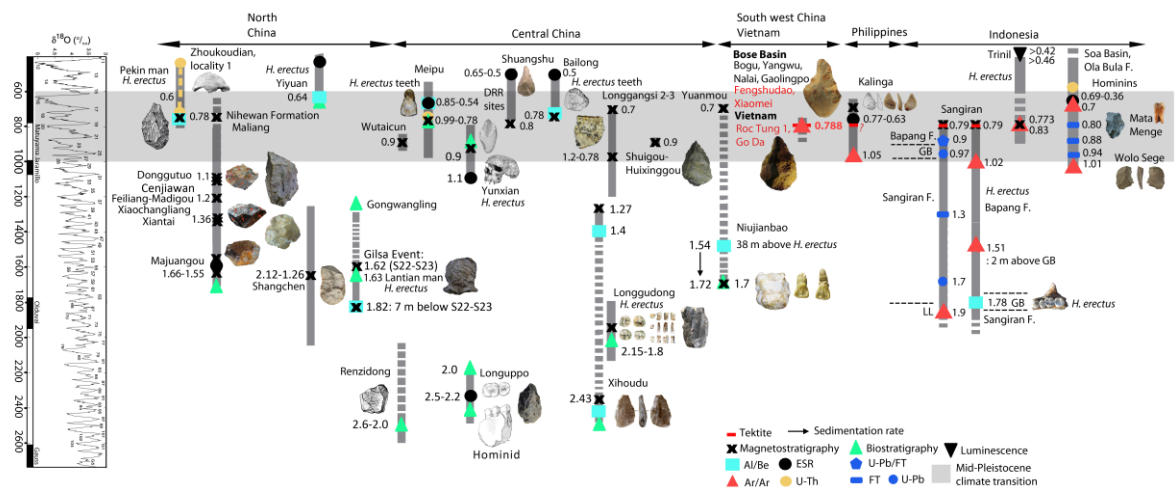
993 Figure 1

994

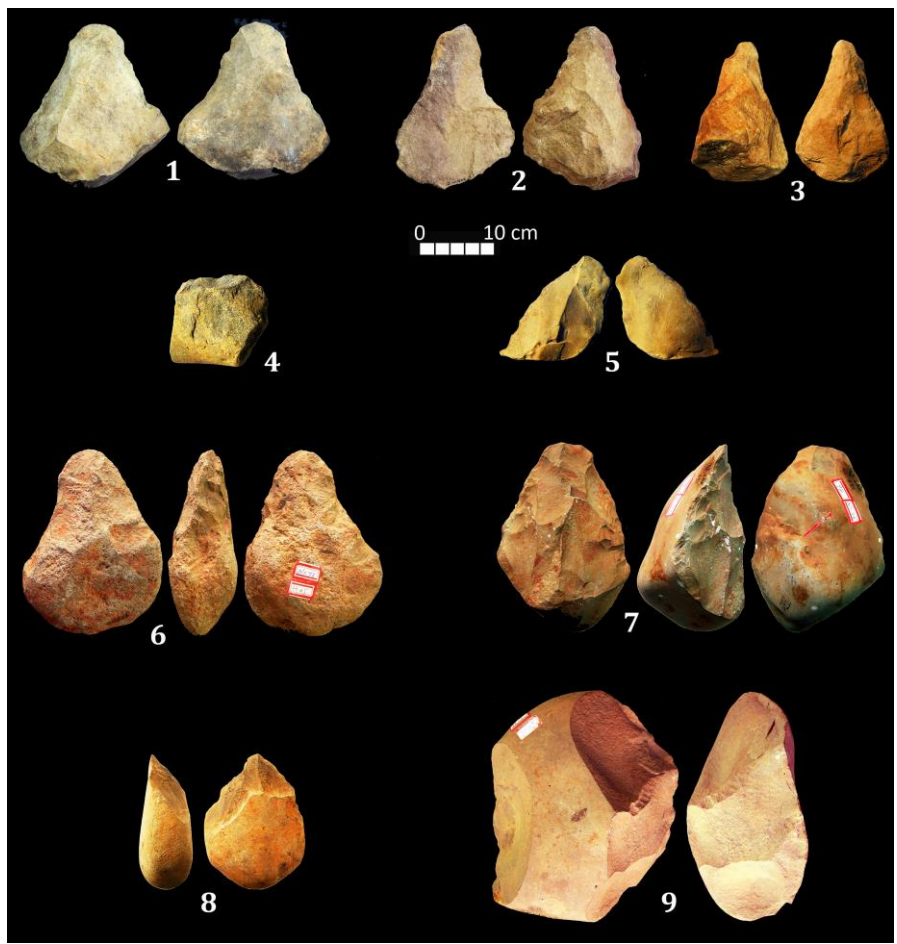
995 70°E 80°E 90°E 100°E 110°E 120°E 130°E 140°E



1019
1020 Figure 2



1038 Figure 3



1069

1070 Figure 4



1071

1072

1073 Figure 5

1074

1075

1076

1077

1078

1079

1080

1081

1082

1083

1084

1085

1086

1087

1088

1089



1090

1091 Figure 6

1092

1093

1094

1095

1096

1097

1098

1099

1100

1101

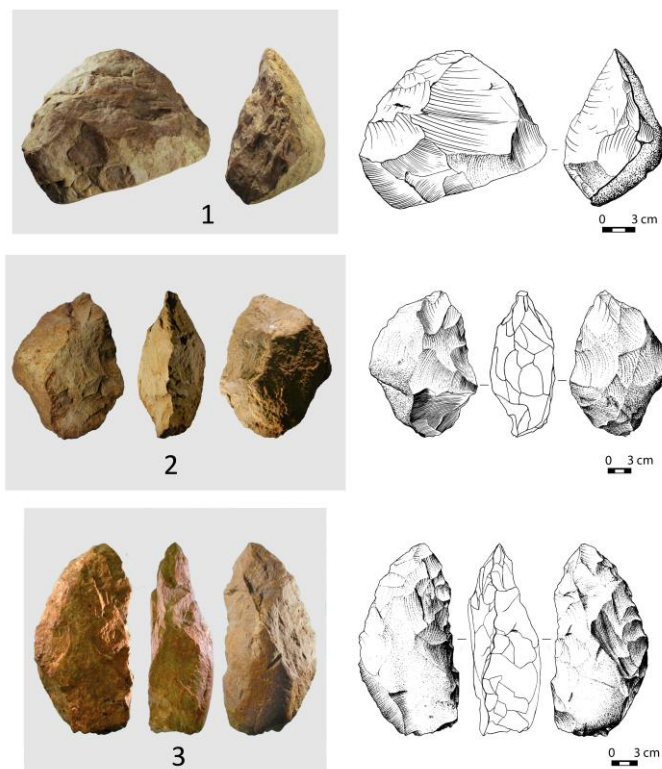
1102

1103

1104

1105

1106



1107
 1108
 1109
 1110
 1111
 1112
 1113
 1114
 1115
 1116
 1117
 1118
 1119
 1120
 1121
 1122
 1123
 1124
 1125
 1126
 1127
 1128
 1129
 1130
 1131
 1132
 1133
 1134
 1135
 1136
 1137
 1138
 1139
 1140
 1141
 1142
 1143
 1144
 1145
 1146
 1147
 1148
 1149
 1150
 1151
 1152
 1153
 1154
 1155
 1156

Figure 7

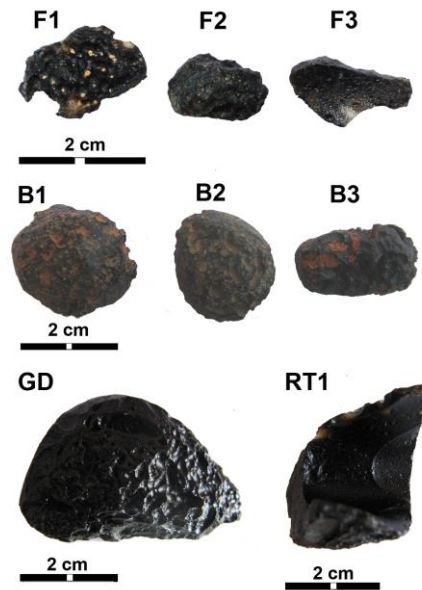
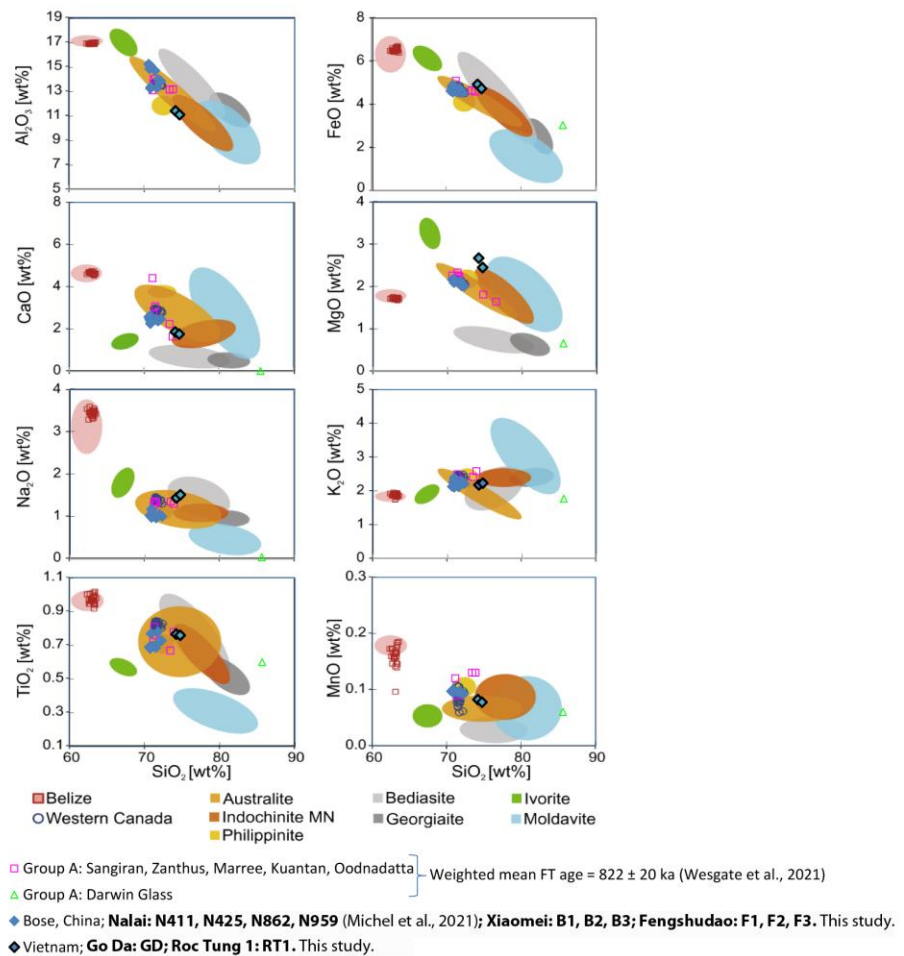
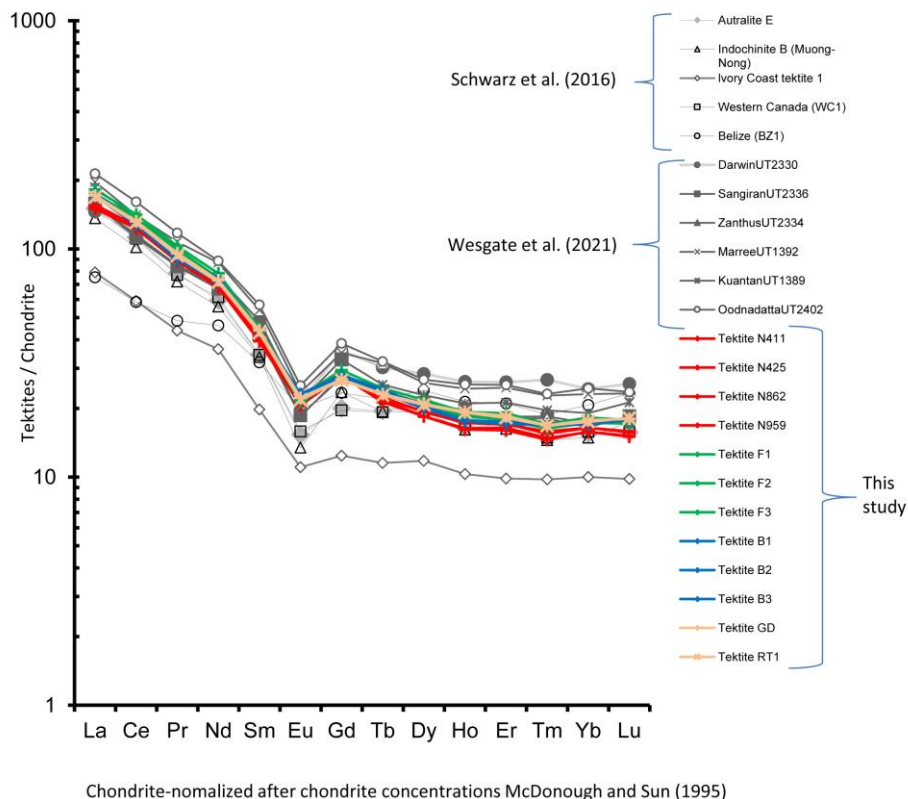


Figure 8



1157
1158 Figure 9



1184 Figure 10

